Proceedings of the 20th International Conference on Soil Mechanics and Geotechnical Engineering– Rahman and Jaksa (Eds)

Evaluation of pore pressure prediction models from centrifuge tests in liquefiable soils

Évaluation de modèles de prévision de la pression interstitielle par des essais en centrifugeuse in sols liquéfiables

António Viana da Fonseca & Sara Rios
CONSTRUCT-GEO, Dep. of Civil Engineering, Faculty of Engineering, University of Porto, Portugal, viana@fe.up.pt

Maxim Millen
Department of Civil and Natural Resources Engineering, Faculty of Engineering, University of Canterbury, New Zealand

ABSTRACT: Buildings located on liquefiable soil deposits can experience damage during earthquakes from both the dynamic ground shaking and the permanent ground deformations due to a build-up of excess pore pressure in the soil (liquefaction). These two effects are related since the reduction of soil stiffness, modifies its dynamic response. The expected damage is dependent on the amount of seismic energy reaching the ground surface before liquefaction. Simplified liquefaction assessment methods to estimate pore pressure build up are very important, and centrifuge tests are an excellent opportunity to validate them. In this paper two methods, one based on the equivalent cyclic stress and another based on the cumulative strain energy, were used to predict the pore pressure build up in a series of centrifuge tests. The results showed that both methods provided moderate estimates of the time of liquefaction. For the sensors measuring a pore pressure ratio (r_u) higher than 0.7, the amount of seismic energy (Arias Intensity) released at the base motion sensor before reaching r_u=0.7 was compared between the centrifuge and the two models. The percentage of cases within the 1:2 and 2:1 bounds was 46% for the stress based method and 62% for the strain energy based method.

RÉSUMÉ: Bâtiments construit dans sols liquéfiables peut souffrir dommages pendant tremblements de terre résultant de la combinaison de l'excitation séismique et/ou de l'incrément de pression interstitielle dans le sol (liquéfaction). Ces deux effets sont liés parce que la réduction de la rigidité du sol, modifie sa réponse séismique. Le dommage attendu est dépendent de la quantité d'énergie séismique qui arrive à la surface avant la liquéfaction. Méthodes simplifiés de prévision de la liquéfaction estimant l'incrément de pression interstitielle sont très importants, et les résultats d'essais en centrifugeuse sont une excellente opportunité pour les valider. Dans ce travail deux méthodes, un basée dans la contrainte cyclique équivalent et l'autre basée dans l'énergie de déformation accumulé, ont été utilisées pour prédire l'incrément de pression interstitielle dans une série d'essais en centrifugeuse. Les deux modèles présentent estimatives acceptables du temps de liquéfaction. Pour les capteurs détectant un ratio de pression interstitielle supérieur (r_u) à 0.7, la quantité d'énergie séismique (Intensité d'Arias) mesuré à la base avant r_u=0.7 a été comparé entre les résultats de la centrifugeuse et les deux modèles. Le pourcentage de cas entre les limites de 1:2 et 2:1 a été de 46% pour le méthode basé dans la contrainte et 62% pour le méthode basé dans l'énergie de déformation.

KEYWORDS: liquefaction, centrifuge tests, stress-based methods, energy-based methods, time of liquefaction

1 INTRODUCTION

Earthquake induced soil liquefaction may led to significant damage in structures and infrastructure founded on potentially liquefiable soils, as observed in Adapazari, Turkey, during 1999 Kocaeli earthquake (Bray et al., 2004), in Christchurch, New Zealand (Cubrinovski et al., 2011; Bray et al., 2017), or in Japan during 2011 Tohuko earthquake (Yamaguchi et al., 2012). These phenomena become visible at the surface through the permanent deformations namely: settlements in shallow foundations (including differential settlements causing building rotation); lateral displacements (whose magnitude can be considerable in slopes, earth retaining structures, or levees close to waterlines, but also in horizontally loaded foundations); or sand boils (often causing heave and failure of critical infrastructures such as electricity, clean and waste water, communications, etc..).

During LIQUEFACT project (www.liquefact.eu) a rational methodology was developed to estimate damage in buildings founded in ground masses susceptible to earthquake induced liquefaction. This methodology, developed for reinforced concrete buildings on shallow foundations over layered soil profiles, is a modular approach based on soil-structure interaction system, considering the soil as part of the model, instead of considering liquefaction as a hazard (Viana et al., 2018, Millen et al., 2019).

In areas susceptible to liquefaction, a strong focus on damage related to soil and foundation deformation is usually assumed, disregarding the damage associated to strong ground shaking, justified by the natural isolation that can occur due to the weakening of the soil during liquefaction (Millen et al. 2018).

However, complete liquefaction does not occur instantly at the beginning of shaking (e.g. Wildlife record from the 1987 Superstition Hills earthquake, Kramer et al., 2011), and therefore the building can be exposed to intense shaking prior to liquefaction or while the soil is in a semi-liquefied state.

For this reason, an estimation of the amount of seismic energy that reaches the ground surface before liquefaction occurs is important for the prediction of building damage. This can be assessed with an intensity measure such as Arias Intensity (Kayen and Mitchell, 1997).

Nonlinear effective stress numerical analysis is a fully-coupled option to estimate the role of liquefaction on the extent of seismic energy propagation. However, these approaches require the calibration of an important number of geotechnical parameters. Alternative, widely used simplified methods have been developed to estimate the factor of safety in relation to liquefaction triggering but do not provide an estimate of the propagation of seismic energy. It is therefore important to develop and validate simplified methods that can improve the estimation of the seismic energy reaching ground surface before liquefaction. Centrifuge tests can be a good opportunity to

validate those methods, although it is recognized that centrifuge tests do not completely represent reality and therefore, adjustments are needed to compare to in situ conditions.

This work applies two simplified methods to predict the seismic energy reaching ground surface before liquefaction in a series of centrifuge tests performed in ISMGEO (Italy) during the LIQUEFACT project (www.liquefact.eu). One is based on the classical estimation of the equivalent cyclic shear stress, assuming a rigid body behavior, while the other is innovatively based on the principles of energy conservation, particularly the strain energy. The soil liquefaction resistance, in terms of strain energy and cyclic shear stress, was defined based on cyclic triaxial tests of the same soil.

2 SIMPLIFIED METHODS TO PREDICT THE TIME OF LIQUEFACTION

2.1 *Method based on the equivalent cyclic stress*

This method is based on the procedure proposed by Seed et al. (1975) and further developed by others (eg., Boulanger and Idriss, 2012, 2016). These authors have provided a simple liquefaction triggering assessment method, which has been widely used throughout the world. The factor of safety results from the ratio between the cyclic resistance ratio (*CRR*) of the soil and the cyclic stress ratio (*CSR*) applied by the earthquake. The *CRR* can be obtained directly from laboratory tests, as cyclic triaxial tests or cyclic simple shear tests, or by empirical correlations with in situ tests such as SPT or CPTU tests. The *CSR* is a ratio between the cyclic shear stress and the vertical effective stress at rest. Given that ground shaking is irregular, the seismically induced shear stress has to be converted into an equivalent uniform *CSR*. It has been assumed that the equivalent uniform loading has a cyclic stress ratio based off 0.65 of the maximum peak acceleration at the ground surface (*PGA*) and converted to an equivalent number of cycles corresponding to a magnitude 7.5 event by the *MSF* parameter, as indicated in equation (1)

$$CSR_{M=7.5} = 0.65 \cdot PGA \cdot \frac{\sigma_{v0}}{\sigma'_{v0}} r_d \frac{1}{MSF} \quad (1)$$

Where σ_{v0} and σ'_{v0} represent, respectively, the total and effective stress at rest; r_d is the shear stress reduction factor, and *MSF* is the magnitude scaling factor. r_d was calculated by equations (2), (3) and (4) proposed by Idriss (1999) as a function of magnitude (M) and depth (z):

$$r_d = e^{[f(z)+g(z)\cdot M]} \quad (2)$$

$$f(z) = -1.012 - 1.126 \cdot sin\left(\frac{z}{11.73} + 5.133\right) \quad (3)$$

$$g(z) = 0.106 + 0.118 \cdot sin\left(\frac{z}{11.28} + 5.142\right) \quad (4)$$

For the estimation of the pore pressure build up during the earthquake, which may eventually cause soil liquefaction, Booker et al. (1976) have proposed equation (5) for the pore pressure ratio (r_u) defined as the ratio between the excess pore pressure generated and the vertical effective stress at rest.

$$r_u = \frac{2}{\pi} arcsin\left[\left(\frac{N}{N_L}\right)^{1/2\beta}\right] \quad (5)$$

Where N is the number of uniform cycles, N_L is the number of uniform cycles required to liquefaction and β is an empirical coefficient which can be determined by the following proposal of Polito et al. (2008):

$$\beta = c_1 FC + c_2 Dr + c_3 CSR + c_4 \quad (6)$$

Where *FC* is the soil fines content, *Dr* is the soil relative density and c_1, c_2, c_3 and c_4 are regression constants, which vary with the fines content. For *FC*<35%: c_1 =0.01166; c_2=0.007397; c_3=0.01034; and c_4=0.5058; while for *FC*≥35%: c_1=0.002149; c_2=−0.0009398; c_3=1.667; and c_4=0.4285.
The number of uniform equivalent cycles can be obtained by the power law between the normalized cyclic stress and the number of cycles to liquefaction (equation (7)), although the exponent *b* may have a huge variation (Boulanger and Idriss, 2014).

$$CSR = a.N^{-b} \quad (7)$$

So, for two cycles with CSR_A and CSR_B the number of relative cycles causing liquefaction can be easily obtained by expression (8). Assuming a reference value for the number of equivalent cycles corresponding to a magnitude of 7.5 (M=7.5), the ratio between CSR_A and CSR_B corresponds to the definition of the magnitude scaling factor:

$$\frac{N_A}{N_B} = \left(\frac{CSR_B}{CSR_A}\right)^{1/b} \Leftrightarrow MSF = \frac{CSR_M}{CSR_{M=7.5}} = \left(\frac{N_{M=7.5}}{N_M}\right)^b \quad (8)$$

In this work, equation (5) was implemented considering that the N/N_L ratio can be calculated by equation (9), using a N_{ref} of 15 cycles, which was the value that Idriss (1999) indicates for the magnitude of 7.5. The value of *CSR* was calculated by equation (10) where a peak counting method (counting the maximum peak between two points crossing the xx axis) was used to identify the acceleration peaks (acc_{peaks}).

$$\frac{N_L}{N} = \sum N_{ref} \cdot \left(\frac{CRR}{CSR}\right)^{1/b} \quad (9)$$

$$CSR = \left|acc_{peaks}\right| \cdot \frac{\sigma_{v0}}{\sigma'_{v0}} \cdot r_d \quad (10)$$

To calculate the soil resistance, the *CRR* for 15 cycles to liquefaction (CRR_{15}) was corrected by the overburden correction factor (K_σ), defined by equation (11) from Boulanger and Idriss (2014) where C_σ is given by equation (12) with q_{c1Ncs} = 90 back calculated from a relative density of 50% using equation (13) from Idriss and Boulanger (2008):

$$K_\sigma = 1 - C_\sigma ln\left(\frac{\sigma'_v}{P_a}\right) \leq 1.1 \quad (11)$$

$$C_\sigma = \frac{1}{37.3 - 8.27(q_{c1Ncs})^{0.264}} \leq 0.3 \quad (12)$$

$$D_R = 0.465\left(\frac{q_{c1Ncs}}{0.9}\right)^{0.264} - 1.063 \quad (13)$$

2.2 *Method based on the cumulative strain energy*

To overcome some of the limitations of the method based on equivalent cycle stress, several energy-based methods have been developed using dissipated energy (Davis and Berril, 1982; Green et al., 2000; Kokusho, 2013) and more recently using strain energy (Millen et al., 2020). These methods avoid:

- Instant parameters such as PGA, favoring cumulative seismic intensity measures, allowing a full time series evaluation;
- the conversion to a uniform equivalent loading, since energy based methods are considered independent of the load amplitude.

In particular, the method proposed by Millen et al. (2020) is based on the cumulative absolute strain energy (*CASE*, or *NCASE* when normalized by the vertical effective stress at rest)

defined as the cumulative change in absolute peak strain energy. *CASE* can be computed as the sum of the absolute change in strain energy between the strain energy peaks in the response (equation 14).

$$CASE = \sum_{j=0}^{n_{peaks}} |\tau_{average,j}| \cdot |\gamma_{j+1} - \gamma_j| \quad (14)$$

where τ is the shear stress and γ is the shear strain and j is the successive peak strain energy points.

In the estimation of the seismic demand, the *NCASE* demand at a certain depth ($NCASE_{z=h}$) is approximated using the nodal surface energy spectrum (equation 15). $NCASE_{u,\xi=0}$ is the *NCASE* at a depth h, for a homogeneous linear soil deposit with zero damping; $\eta_{z=h}$ is a reduction factor to account for damping; and $G_{z=h}/G_{input}$ is the ratio of shear modulus at depth, h, compared to the shear modulus where the input ground motion is defined. $NCASE_{u,\xi=0}$ is computed with equation 16 as the cumulative change in absolute kinetic energy of the equivalent strain motion divided by the initial vertical effective stress, σ'_{v0} where $\dot{u_{s,i}}$ is the velocity of the equivalent strain motion at time, i, and ρ is the mass density. The equivalent strain motion is computed using equation (17) as the difference between the upward and downward motion at depth, h, which is the same motion shifted by a time interval, shift t, corresponding to the travel time from h to the surface and back. The damping reduction factor $\eta_{z=h}$ is the expected level of reduction in amplitude at depth, h, due to damping, as computed in equation (18), where η_{total} is the ratio of the amplitude of the upward going wave at the surface compared to at the base, and t_h is the travel time from the surface to the depth, h. Finally, η_{total} is calculated in equation (19), where ξ is the small strain damping, taken as the default of 0.03, and f_e is the energy frequency of the ground motion, with a default value of 2 Hz.

$$NCASE_{z=h} = \mathrm{NCASE}_{u,\xi=0} \cdot \eta_{z=h} \cdot \frac{G_{z=h}}{G_{input}} \quad (15)$$

$$NCASE_{u,\xi=0} = \frac{\rho}{\sigma'_{v0}} \cdot \sum_{i=1}^{n} |\Delta(\dot{u_{s,i}} \cdot |\dot{u_{s,i}}|)| \quad (16)$$

$$\ddot{u}_{ts,i} = \ddot{u}_i - \ddot{u}_{i+shift\ t} \quad (17)$$

$$\eta_{z=h} = \eta_{total} + (1 - \eta_{total})/2 \cdot t_h/t_H \quad (18)$$

$$\eta_{total} = \exp(-\xi \cdot t_H \cdot 2 \cdot \pi \cdot f_e)^2 \quad (19)$$

The *NCASE* demand throughout the depth is then calculated from the nodal surface energy spectrum (*NSES*) which provides an exact solution for the cumulative absolute strain and kinetic energy in a linear homogenous soil profile. Simple corrections were developed by Millen et al. (2020) to account for soil damping and changes in soil shear stiffness.

For the application of this method to the prediction of pore pressure build up, a simple expression was proposed by Millen et al (2020), although it is recognized that this expression may depend on the type of soil:

$$r_{u,i} = \min\left(\sqrt{\frac{NCASE_i}{NCASE_{liq}}} \cdot r_{u,liq}; 1.0\right) \quad (20)$$

Where $NCASE_i$ corresponds to the *NCASE* demand that arrives to a given soil layer due to the seismic excitation and $r_{u,liq}$ corresponds to the pore pressure ratio at the time of liquefaction triggering, generally based on double amplitude axial strain, effective vertical stress of simply a pre-defined value of r_u (0.9, 0.95 or 0.98). $NCASE_{liq}$ corresponds to the *NCASE* necessary for soil liquefaction, being therefore a measure of soil resistance, such as *CRR*, with the additional advantage of being constant with stress amplitude but sensitive to soil properties.

3 LIQUEFACTION RESISTANCE FROM LABORATORY TESTS

To facilitate a comparison between the different pore pressure methods and the centrifuge tests described in the next section, the soil liquefaction resistance in terms of CRR_{15} and $NCASE_{liq}$ can be obtained from laboratory tests. Figure 1 shows the CSR curves for Ticino Sand. Liquefaction triggering was considered for an effective vertical stress of 7 kPa calculated by equation (21) where $\sigma'_{v,liq}$ is 7 kPa.

$$r_{u,liq} = \frac{\sigma'_v - \sigma'_{v,liq}}{\sigma'_v} \quad (21)$$

Based on this data, equation (7) was adjusted using a b value of 0.34 as suggested by Idriss (1999). This procedure returned CRR_{15} equal to 0.17, 0.16 and 0.22 for relative densities of 49%, 54% and 57%. A value of CRR_{15} =0.17 was therefore taken to represent the soil in the centrifuge tests which were all near a relative density of 50%, consistent with Bilotta et al. (2019) and Ozcebe et al. (2021). The same parameter b was used in equations (7), (8) and (9) and for the calculation of β equation (6) was used assuming zero fines content since Ticino Sand is a clean sand.

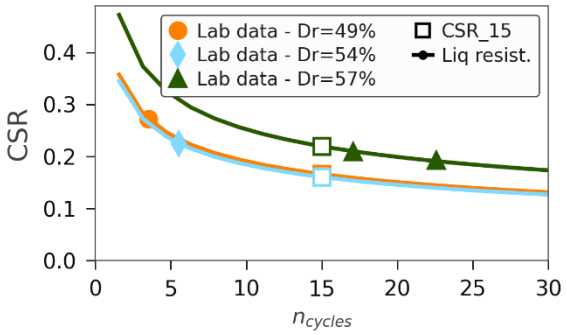

Figure 1. Curves *CSR* versus number of cycles to liquefaction for a liquefaction criterion of 7 kPa of effective stress. The square symbol represents the CSR_{15}

For the method based on the cumulative strain energy the soil resistance is measured by $NCASE_{liq}$, whose values were obtained from the Fioravante and Giretti (2016) data. Figure 2 shows the relation of $NCASE_{liq}$ with CSR for the same liquefaction criterion of 7 kPa of effective stress. There was a notably variation in $NCASE_{liq}$ shown in Figure 2 and value of 0.025 was assumed.

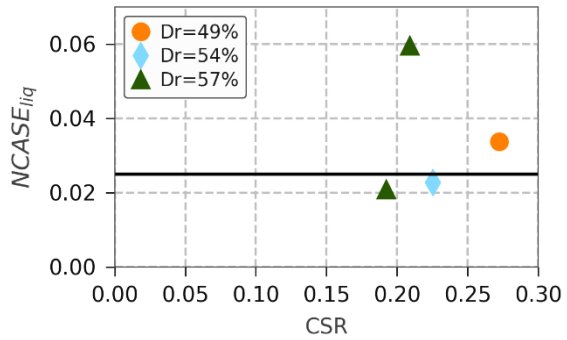

Figure 2. $NCASE_{liq}$ from the cyclic triaxial tests on Ticino Sand performed by Fioravante and Gireti (2016) calculated for a liquefaction criterion corresponding to an effective stress of 7 kPa

Additionally, the shear modulus was considered stress dependent according to equation (22),

$$\mathrm{G} = G_0 \cdot p_{atm} \cdot \sqrt{p'/p_{atm}} \quad (22)$$

where, G_0 was taken as 624 according to Bilotta et al. (2019), p_{atm} is the atmospheric pressure and p' is the mean effective stress.

4 ISMGEO CENTRIFUGE TESTS

4.1 *Description of the tests*

The centrifuge tests analyzed in this work were performed during LIQUEFACT project (www.liquefact.eu) at the ISMGEO laboratory (Instituto Sperimentale Modelli Geotecnici, in Italy). The soil profiles of the tested models had 15 m of homogeneous saturated loose sand sometimes topped by an overconsolidated clay layer. In those models, the following sensors were placed: acceleration sensors, pore pressure sensors, and displacement sensors. The differences between the models concern the applied ground motions, as well as the soil used and the presence or not of structures or mitigation measures such vertical drains. Descriptions of the tests and procedures can be found in Airoldi et al. (2018a).

Most tests were performed with Ticino Sand, a well known Italian uniform medium to coarse sand, with angular and subrounded particles, composed by 30% quartz, 65% feldspar and 5% mica (Fioravante & Giretti, 2016). The preparation of the sand layer comprised dry pluviation in the Equivalent Shear Beam (ESB) container from a very small constant height around 3 cm, calibrated to obtain a relative density of 40% (which increases with the following procedures to around 50%). In some models, the top layer was made of Pontida Clay, a low plasticity kaolinitic silty clay, previously overconsolidated in a consolidometer and then placed above the sand layer as described by Airoldi et al. (2018a).

The model was geometrically scaled down by a factor of N=50 and the models were subjected to a centrifugal acceleration of 50g. In dynamic phenomena (as excess pore pressure generation) the time scale factor is N while in consolidation/seepage phenomena (as the excess pore pressure dissipation) the time scale factor is N^2. To overcome this problem, the models were saturated with a fluid 50 times more viscous than water, using a solution of water and hydroxypropyl methylcellulose (HPMC).

4.2 *Data treatment*

The raw data of the centrifuge tests results (Airoldi et al., 2018b) was treated in order to convert the units from model to prototype. The scale factor to convert the model units to prototype was N=50 according to the acceleration of the centrifuge. The scaling ratios for the main parameters analyzed was: Time [t·N], Acceleration [a/N], Stress [N], Displacement [d·N]. Since a fluid, more viscous than water was used for the model saturation, a single scaling ratio was used for the time variable.

On the acceleration records, it was necessary to remove the first 5 seconds in order to correct smaller errors related with equipment calibration and possible inclination of the sensors before the seismic event. Additionally, a 4th order Butterworth high pass filter of 0.1 Hz and a low pass filter of 20 Hz were used. The first aims at removing problems related with sensor inclination during the test and the second removes any high frequency noise related with the measurement device. The records were also cut to leave only the portion where shaking occurred together with 10 seconds before and 20 seconds after. As the record had a faint oscillating background acceleration, this trimming caused a bias acceleration at the start resulting in a non-zero average velocity. This was removed by calculating the acceleration, and then removing it over a two second window at the start of the record with an initial acceleration of zero. The data presented herein always refers to the prototype units converted as indicated above.

5 COMPARISON BETWEEN SIMPLIFIED METHODS AND CENTRIFUGE TESTS

5.1 *Sensors and parameters for the comparative analysis*

To facilitate a fair comparison between the simplified methods and the centrifuge tests only a subset of the pore pressure transducers were used. There were three reasons for excluding sensors from the comparison, first was that the sensor should represent free-field conditions away from buildings and mitigation methods that were included in some of the centrifuge tests. Second was sensors that were located near the model base, where the significant stiffness contrast invalidated the assumptions used for computing the demands (since the simplified methods rely on demand estimates from the ground surface, whereas this comparison relied on demand estimates using the base input motion). The third set of sensors that were excluded were sensors near the surface, due to difficulties in obtaining the capacity at very low confining stresses and sensors near the surface exhibited significant vertical water seepage (Fioravante et al., 2019, Rios et al., 2020). This selection resulted in 56 sensors that were used in the following analysis.

The full exclusion criteria are listed below:

- Sensors located at a depth corresponding to $\sigma'_v < 15$ kPa;
- Sensors located in the clay layer;
- Sensors located immediately below buildings or very close to liquefaction mitigation measures;
- Sensors that did not register any pressure due to technical problems.

The stress based method uses the expected surface excitation, and estimates the shear stresses at depth using a rigid body assumption with depth correction factor based on the earthquake magnitude, assuming that seismic excitation is based on total stresses behavior (i.e., without liquefaction). However, since most tests did not record the surface acceleration, or the soil column developed considerable excess pore pressure, the surface acceleration could not be used to estimate the demand in many tests. Therefore, the base seismic excitation was assumed equal to the surface acceleration and it was used instead, with the depth correction factor applied based on the magnitude of the recorded earthquake input motion. This hypothesis was validated using tests 4 to 9 where both the base and surface acceleration were recorded but liquefaction did not occur. For those six tests, the CSR for the magnitude of 7.5 (CSR_{15}) was calculated for the base and surface motions. The ratio between the calculated CSR_{15} from the surface over the base seismic excitations for each of the six tests was the following: 0.87, 1.25, 1.23, 0.91, 1.19 and 1.02.

The strain energy method developed by Millen et al. (2020) uses the upward motion either at the base or surface, but it was developed for soil profiles that had only minor variations in shear modulus between layers. However, the centrifuge tests had a metallic base (essentially a rigid base). Therefore, the influence of the impedance contrast between the soil and the metallic base had to be limited. Tests 4 to 9 were used again to determine the limiting factor of 2 to account for the shear modulus variation. This was achieved by equating the demand calculated from the surface acceleration, with the demand calculated from the base. Using the limiting factor of 2, the ratio between surface and base energy for the six tests was 1.00, 1.63, 1.26, 0.83, 1.39, 0.91 respectively. The limiting factor of 2 was applied to all subsequent tests.

5.2 *Comparison of pore pressure evolution*

Figure 3 presents the comparison between the pore pressure measured in the centrifuge tests with the pore pressure build up estimated by the simplified methods for one of the tests. This test was chosen since it does not include any buildings or liquefaction mitigation measures, and the selected pore pressure sensor was located at the middle of the sand layer. In Figure 3b) there is also

the base seismic excitation measured by the corresponding sensor.

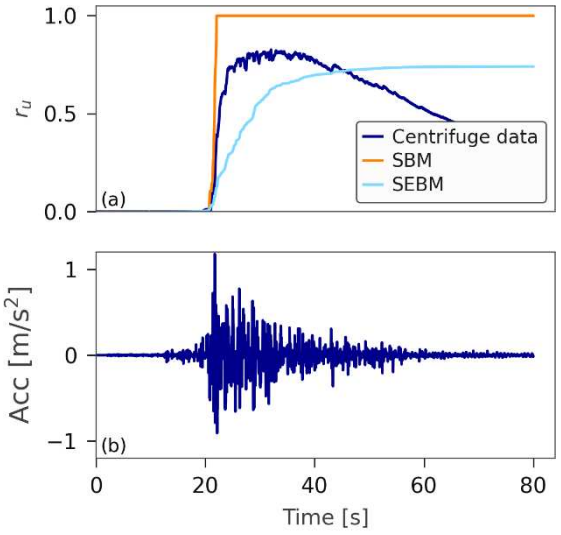

Figure 3. a) Comparison of the pore pressure evolution predicted by the simplified methods with the measured values in the centrifuge test number 3; b) input acceleration

Although these methods have different base hypothesis, they provide reasonable estimation of pore pressure build up. However, the rapid drainage that was observed in the centrifuge tests as well as the natural isolation had a significant influence on the pore pressure evolution that was not accounted for in the simplified methods.

5.2 *Comparison of pore pressure build-up*

A comparison of all 56 selected sensors was performed to evaluate the efficacy of the two prediction models. Since many tests did not reach liquefaction, and others suffered from rapid drainage, the evaluation was split into two categories. Category A consisted of all sensors where r_u>0.7 (26 sensors), and Category B contained the remainder (19 sensors). In Category A the amount of seismic energy (Arias Intensity) released at the base motion sensor before reaching r_u=0.7 was compared between the centrifuge and the two models (example shown in Figure 4a)). Arias Intensity was considered a more indicative proxy from time of liquefaction, rather than using the absolute time which contains an arbitrary length of no shaking at the start. For Category B, the maximum r_u value from the centrifuge test is compared against the r_u from each model at the same time instance (example shown in Figure 4b).

Figure 5 presents the comparison of the centrifuge tests with the simplified methods, for the two categories identified above, respectively in Figure 5a) for the cases where the sensor r_u >0.7, and in Figure 5b) for the cases where the sensor r_u<0.7. It becomes clear from the graphs that SBM method tended to be more conservative than SEBM, as the method often estimated liquefaction in cases where it did not happen. For Category A, the SBM has 46% of the cases within the 1:2 and 2:1 bounds while SEBM has 62%. For Category B, the number of cases within the 1:2 and 2:1 bounds is 53% and 95% for SBM and SEBM respectively. However, it should be highlighted that the soil capacity was estimated in both methods with a reduced number of element tests. The accuracy of the methods could be improved if a better characterization of the soil was available.

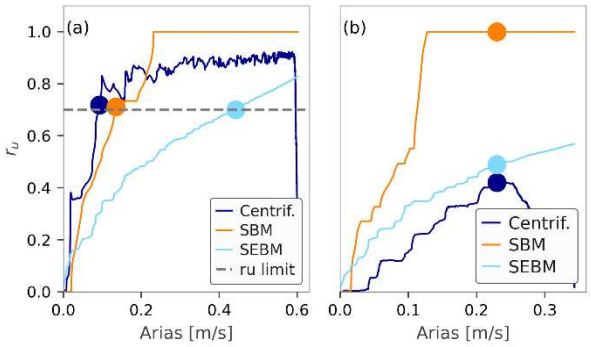

Figure 4. Comparison of the two simplified methods and the centrifuge data in a test where $r_u^{centrifuge} > 0.7$ (a) and in a test where $r_u^{centrifuge} < 0.7$ (b). The name of the sensor selected for comparison was PPT-FF-L1TC-M

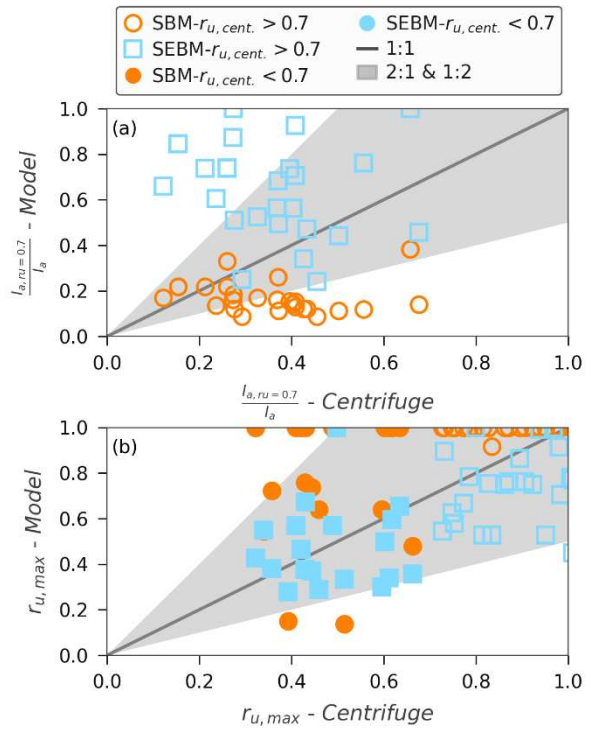

Figure 5. Comparison of the two simplified methods the centrifuge data for the cases where $r_u^{centrifuge} > 0.7$ (a) and for the cases where $r_u^{centrifuge} <$ 0.7 (b)

6 CONCLUSIONS

In this work, two simplified methods are evaluated by estimating the Arias Intensity in a series of centrifuge tests performed at ISMGEO, Italy. One of the methods was based on the equivalent cyclic stress following the ideas of Seed et al (1975) and others (e.g., Boulanger and Idriss, 2016). The other method was based on the accumulated strain energy as proposed by Millen et al. (2020). The advantage of energy based methods is the possibility to integrate all seismic spectra avoiding the conversion to a equivalent uniform loading, and the use of representative parameters (such as PGA, peak ground acceleration). As most centrifuge tests were performed on Ticino Sand, the cyclic resistance of this sand was evaluated by the interpretation of cyclic triaxial tests performed by Fioravante and Giretti (2016). The SBM method tended to be a bit conservative, as the method often predicted liquefaction when it did not happen. Still, on the strain energy method there are issues that need further

improvement: 1) the difficulty to estimate $NCASE_{demand}$ of a rigid base requires further theoretical development to better constrain the estimates, 2) the variation in $NCASE_{capacity}$ at different vertical effective stresses needs to be evaluated, 3) the build up of pore pressure with *NCASE* needs to be better understood.

6 ACKNOWLEDGEMENTS

LIQUEFACT project (Assessment and mitigation of liquefaction potential across Europe: a holistic approach to protect structures/infrastructures for improved resilience to earthquake-induced liquefaction disasters) has received funding from the European Union's Horizon 2020 research and innovation programme under grant agreement GAP-700748. This work was financially supported by: Base Funding - UIDB/04708/2020 of the CONSTRUCT - Instituto de I&D em Estruturas e Construções - funded by national funds through the FCT/MCTES (PIDDAC). The authors would like to acknowledge the availability of centrifuge data, namely to Professor Vincenzo Fioravante and Doctor Sergio Airoldi who led the team responsible for these tests. In addition, we also acknowledge Professor Vincenzo Fioravante and Doctor Daniela Giretti for supplying the cyclic triaxial test data from which it was possible to obtain reliable values of Ticino Sand.

7 REFERENCES

Airoldi, S., Fioravante, V., Giretti, D., & Moglie, J. 2018b. Validation of liquefaction retrofitting techniques from geotechnical centrifuge small scale models [Data set]. Zenodo. http://doi.org/10.5281/zenodo.1281598

Airoldi, S., Fioravante, V., Giretti, D., and Moglie, J. 2018a. Deliverable D 4.2 - Report on validation of retrofitting techniques from small scale models. LIQUEFACT Project, Horizon 2020 European Union funding for Research & Innovation, GA. Nº: 700748 (www.liquefact.eu)

Bilotta, E., Chiaradonna, A., Fasano, G., Flora, A., Mele, A., Nappa V., Lirer, S., Fioravante, V. 2019. Experimental evidences of the effectiveness of some liquefaction mitigation measures. *IABSE Symposium Towards a Resilient Built Environment - Risk and Asset Management*, Guimarães, Portugal

Booker, J. R., Rahman, M. S., & Seed, H. B. 1976. GADFLEA— A computer program for the analysis of pore pressure generation and dissipation during cyclic or earthquake loading. Rep. EERC 76-24

Boulanger, R. W., & Idriss, I. M. 2012. Probabilistic Standard Penetration Test–Based Liquefaction–Triggering Procedure. *J. of Geotechnical and Geoenvironmental Engineering*, 138(10), 1185–1195.

Boulanger, R. W., & Idriss, I. M. 2016. CPT-Based Liquefaction Triggering Procedure. *Journal of Geotechnical and Geoenvironmental Engineering*, 142(2), 04015065.

Boulanger, R.W. & Idriss, I.M. 2014. CPT and SPT based liquefaction triggering procedures. Report No. UCD/CGM-14/01. *Center for Geotechnical Modeling, University of California, Davis*. 134 pp. http://nees.ucdavis.edu/publications/Boulanger_Idriss_CPT_and_SPT_Liq_triggering_CGM-14-01_2014.pdf

Bray, J. D., Markham, C. S., & Cubrinovski, M. 2017. Liquefaction assessments at shallow foundation building sites in the Central Business District of Christchurch, New Zealand. *Soil Dynamics and Earthquake Engineering*, 92(10), 153–164.

Bray, J. D., R. B. Sancio, T. Durgunoglu, A. Onalp, T. L. Youd, J. P. Stewart, R. B. Seed, O. K. Cetin, E. Bol, M. B. Baturay, C. Christensen and T. Karadayilar 2004. Subsurface Characterization at Ground Failure Sites in Adapazari, Turkey. *Journal of Geotechnical and Geoenvironmental Engineerin*g 130(7): 673-685

Cubrinovski, M., Bray, J., Taylor, M., Giorgini, S., Bradley, B., Wotherspoon, L., Zupan, J. 2011. Soil liquefaction effects in the central business district during the February 2011 Christchurch earthquake. *Seismol. Res. Lett*., 82(6), 893–904

Davis, R., & Berril, J. 1982. Energy dissipation and seismic liquefaction in sands. *Earthquake Engineering & Structural Dynamics*, 10(1), 59–68.

Fioravante, V., D. Giretti, J. Moglie, E. Bilotta, G. Fasano, A. Flora and V. Nappa 2019. Centrifuge modelling in liquefiable ground before and after the application of remediation techniques. Earthquake Geotechnical Engineering for Protection and Development of Environment and Constructions- *Proceedings of the 7th International Conference on Earthquake Geotechnical Engineering*.

Fioravante, V., Giretti, D. 2016. Unidirectional cyclic resistance of Ticino and Toyoura sands from centrifuge cone penetration tests. *Acta Geotech*. 11, 953–968

Green, R. A., Mitchell, J. K., & Polito, C. P. 2000. An Energy-Based Excess Pore Pressure Generation Model for Cohesionless Soils. *Proceeding of the John Booker Memorial Symposium*, 1–9

Idriss, I. M. 1999. An update to the Seed-Idriss simplified procedure for evaluating liquefaction potential. *In TRB Workshop on New Approaches to Liquefaction Publication No. FHWARD- 99-165*. Federal Highway Administration

Idriss, I. M., and Boulanger, R. W. 2008. Soil liquefaction during earthquakes. Monograph MNO-12, Earthquake Engineering Research Institute, Oakland, CA, 261 pp.

Kayen, R.E., Mitchell, J.K. 1997. Assessment of liquefaction potential during earthquake by Arias Intensity. *Journal of Geotechnical and Geoenvironmental Engineering*, 123(12), 1162-1174

Kokusho, T. 2013. Liquefaction potential evaluations: energy-based method versus stress-based method. *Canadian Geotechnical Journal*, 50(10), 1088–1099

Kramer, S., Hartvigsen, A. J., Sideras, S. S., & Ozener, P. T. 2011. Site response modelling in liquefiable soil deposits. In *4th IASPEI - Effects of surface geology on seismic motion* (pp. 1–12)

Millen, M., Quintero, J., Panico, F., Pereira, N., Romão, X., Viana da Fonseca, A. 2019. Soil-foundation modelling for vulnerability assessment of buildings in liquefied soils. *7th International Conference on Earthquake Engineering,* Rome, Italy, pp.717-726

Millen, M., Rios, S., Quintero, J. and Viana da Fonseca, A. 2020. Prediction of time of liquefaction using kinetic and strain energy. *Soil Dynamics and Earthquake Engineering*, 128, 1-14

Millen, M., Viana da Fonseca, A., Romão, X. 2018. Preliminary displacement-based assessment procedure for buildings on liquefied soil. *16th European Conference on Earthquake Engineering,* Thessaloniki, 18-21 June

Ozcebe, A.G., Giretti, D., Bozzoni, F., Fioravante, V., Lai, C. 2021. Centrifuge and numerical modelling of earthquake-induced soil liquefaction under free-field conditions and by considering soil–structure interaction. *Bulletin of Earthquake Engineering* 19:47–75

Polito, C. P., Green, R. A., & Lee, J. 2008. Pore Pressure Generation Models for Sands and Silty Soils Subjected to Cyclic Loading. *Journal of Geotechnical and Geoenvironmental Engineering*, 134(10), 1490–1500

Rios, S., Millen, M., Viana da Fonseca, A., Santos, P., Mudanó, P. 2020. Validação de modelos simplificados de previsão do tempo de liquefação através de ensaios de centrifugadora. *Revista Geotecnia*, 148, 31-54

Seed, H., Idriss, I., Makdidi, F., & Nanerjee, N. 1975. Representation of irregular stress time histories by equivalent uniform stress series in liquefaction analyses Report No. EERC 75–29. *Earthquake Engineering Research Center*, University of California Berkeley

Viana da Fonseca, A., Millen, M., Romão, X., Quintero, J., Rios, S., Ferreira, C., Panico, F., Azeredo, C., Pereira, N., Logar, J., Oblak, M., Dolsek, M., Kosic, M., Kuder, S., Logar, M., Oztoprak, S., Kelesoglu, M., Sargin, S., Oser, C., Bozbey, I., Flora, A., Billota, E., Prota, A., Ludovico, M. Chiaradonna, A., Modoni, G., Paolella, L., Spacagna, R., Lai, C., Shinde, S., Bozzoni, F. 2018. Deliverable D 3.2 - Methodology for the liquefaction fragility analysis of critical structures and infrastructures: description and case studies. LIQUEFACT project, Horizon 2020 European Union funding for Research & Innovation, GA nº. 700748 (www.liquefact.eu)

Yamaguchi, Y., M. Kondo and T. Kobori. 2012. Safety inspections and seismic behavior of embankment dams during the 2011 off the Pacific Coast of Tohoku earthquake. *Soils and Foundations* 52(5): 945-955